

A NOVEL WRAPPING CURVELET TRANSFORMATION BASED ANGULAR TEXTURE PATTERN (WCTATP) EXTRACTION METHOD FOR WEED IDENTIFICATION

D. Ashok Kumar¹ and P. Prema²

¹Department of Computer Science, Government Arts College, Tiruchirappalli, India
E-mail: drashoktrichy22@gmail.com

²Department of Agricultural Economics, Agricultural College and Research Institute, Madurai, India
E-mail: pp76@tnau.ac.in

Abstract

Apparently weed is a major menace in crop production as it competes with crop for nutrients, moisture, space and light which resulting in poor growth and development of the crop and finally yield. Yield loss accounts for even more than 70% when crops are grown under unweeded condition with severe weed infestation. Weed management is the most significant process in the agricultural applications to improve the crop productivity rate and reduce the herbicide application cost. Existing weed detection techniques does not yield better performance due to the complex background, illumination variation and crop and weed overlapping in the agricultural field image. Hence, there arises a need for the development of effective weed identification technique. To overcome this drawback, this paper proposes a novel Wrapping Curvelet Transformation Based Angular Texture Pattern Extraction Method (WCTATP) for weed identification. In our proposed work, Global Histogram Equalization (GHE) is used improve the quality of the image and Adaptive Median Filter (AMF) is used for filtering the impulse noise from the image. Plant image identification is performed using green pixel extraction and k-means clustering. Wrapping Curvelet transform is applied to the plant image. Feature extraction is performed to extract the angular texture pattern of the plant image. Particle Swarm Optimization (PSO) based Differential Evolution Feature Selection (DEFS) approach is applied to select the optimal features. Then, the selected features are learned and passed through an RVM based classifier to find out the weed. Edge detection and contouring is performed to identify the weed in the plant image. The Fuzzy rule-based approach is applied to detect the low, medium and high levels of the weed patchiness. From the experimental results, it is clearly observed that the accuracy of the proposed approach is higher than the existing Support Vector Machine (SVM) based approaches. The proposed approach achieves better performance in terms of accuracy.

Keywords:

Global Histogram Equalization (GHE), Adaptive Median Filter (AMF), Convolved Gray Level Co-occurrence Matrix (CGLCM), Wrapping Curvelet Transformation Based Angular Texture Pattern (WCTATP) Extraction Method, Weed Identification

1. INTRODUCTION

The yield of any agriculture products will be vitally affected by the presence of weed and the control of weed leads to a greater yield. The surplus weed can be removed using the herbicides but the excess use can affect the agro-product itself. Weeds are the undesirable plants that can reproduce in the agricultural field and disturb the overall crop yield. Uncontrolled weeds can reduce the crop yield from 10% to about 90%. Hence, weed control is considered as a vital practice in the agricultural systems, to sustain

the crop productivity and quality. In most cases, weed control depends on the usage of chemical herbicides to achieve effective control of weed infestations and obtain high profit. But, the application of chemical herbicides causes adverse effects to the environment and requires more manual labor and expense. If the same types of herbicide are repeatedly applied in the field for the removal of the weeds, there is often a chance of the emergence of weeds to become tolerant to those types of herbicides. This lead to the increasing interest in the development of alternative weed control techniques. To reduce the burden on the agricultural sector, the crop yield should be increased with reduced cost for weed control. Conventionally, a machine vision system can distinguish the crops from the weeds for the effective application of the herbicides and improvement in the crop yield with reduced environmental degradation. An automated system is used in this approach for acquiring the image of different areas of the crop field. Previously, classification of the crops and weeds is performed based on the geometrical characteristics such as leaf shape or plant structure and spectral reflectance characteristics. The ground-based sensor technologies are used to identify the weeds. The development of the computer vision capabilities enables reliable and rapid identification of weeds [1]. Detection of weed using color or shape characteristics is simple and efficient, but the adaptability of this technique is very poor. The weed recognition method using multispectral characteristics is feasible. However it is very expensive.

One of the major problems in crop and weed classification from the agro-product is image acquisition. The input images is taken from the agricultural field under different lighting and environment condition. Another issues in the crop and weed discrimination is the crop and weed grow close together and overlap between plants in the commercial fields. To increase the crop yield accurate detection of weed and herbicide spray is essential.

Several existing approaches addresses the problem of green identification under the assumption that plants show a high level of greenness, but the loss of the greenness due to various reasons such as different lighting conditions are not considered. The efficiency of the weed classification is increased by employing the wavelet transformation [2] techniques for weed discrimination. There are many other research that contributes to the implementation of weed classification such as Fourier transforms [3], Hough transform [4] and linear regression [5]. Although the wavelet transform shows an improved efficiency than all other methods and the wavelet transform itself have some constraints. The classified images from wavelet transform method

have noise in it. Also, the edges in the weed are not classified more accurately due to which the small leaf will be misjudged as weed. No a new techniques such as Curvelet can be used in different application like medial image processing, face recognition. [6] Curvelet texture analysis was used with Support Vector Machine to establish a prediction model for detecting early-stage lung cancer in chest x-ray images.

In this paper, we have introduced a different concept for transformation technique called as Wrapping Curvelet Transformation techniques for crop and weed discrimination. The problem of the edge discontinuity is better approximated by the curvelets than the wavelets. Wrapping curvelet transform is faster computation time and more robust than ridglet and unequally spaced fast Fourier transform. The Wrapping Curvelet Transform has not been used in crop and weed discrimination. To overcome the limitations of the existing weed identification techniques, this paper proposes a novel Wrapping Curvelet Transformation Angular Texture Pattern extraction method are used for weed identification. Adaptive Median Filter is used for filtering the impulse noise from the image and the Global Histogram Equalization (GHE) techniques is used improve the quality of the image. Vegetation pixels are separated from soil and other residue under different lighting conditions using Green pixel extraction (ExG). *k*-means clustering is applied to the filtered image, to cluster the soil and vegetation. Then, the green pixel count of ExG is verified with the pixel count of the clusters. If the green pixel count is nearest to the pixel count of the clusters, then it is considered as the plant image. Wrapping curvelet transformation is applied to the plant image. After applying the curvelet transformation, proposed angular based features are extracted from the transformed image. A Mobility Window Projection (MWP) system represents the movement of the window to each patch of the image. In the texture pattern analysis, the MWP system is used to analyze the variation in the texture. The tamura texture features that correspond to human visual perception. The six textural features (coarseness, contrast, directionality, line-likeness, regularity and roughness) and proposed three features such as Energy, Entropy and Auto-Correlation are extracted from the image, Gabor filter with four orientations is applied to the image and GLCM features are extracted from the Gabor filtered image. PSO-based DEFS approach is applied to select the optimal features. Then, the selected features are learned and passed through a RVM based classifier to find out the weed. Edge detection and contouring is performed for the identification of weed in the plant image. The low, medium and high levels of the weed patchiness are detected using the Fuzzy rule based approach. The proposed approach achieves better performance in terms of accuracy. From the experimental results, it is clearly observed that the accuracy of the proposed approach is higher than the existing SVM-based approaches.

The rest of the paper is organized as follows: Section 2 describes about the existing approaches related to the identification of weeds. Section 3 explains the proposed WCTATP extraction method including the AMF, GHE, vegetation segmentation, curvelet transformation, feature extraction, PSO-based DEFS Feature Reduction, RVM based classification, weed edge detection and contouring and Fuzzy-rule based weed patchiness processes. The performance analysis results of the proposed method are presented in section 4. Section

5 discusses about the conclusion and future scope of the proposed work.

2. RELATED WORK

In the conventional cropping systems, removal of weed was done by applying chemical herbicides on the plants. However, this practice causes adverse effects on the surrounding environment and human health. To reduce the usage of herbicides, the distribution of weeds is sensed automatically by using various approaches. This aids in the optimization of the application dosage of the herbicides in the crop fields. This section explains about various conventional research works and methodologies used for the identification of weed from the plant leaf images.

A novel method for characterizing and recognizing the plant leaves, with the combination of texture and shape features [7]. The Gabor filter and GLCM were used for modeling the texture of the leaf and a set of curvelet transform coefficients was used to capture the shape of the leaf along with the invariant moments. Improved recognition of the leaves with varying texture, size, shape and different orientations was achieved. A machine vision approach for the classification of plants without segmentation and discrimination of the crop and weed [8]. A Random Forest classifier was used for the estimation of crop and weed certainty at sparse pixel positions, instead of segmenting the image [9]. The proposed approach was evaluated using a set of images captured in the organic carrot farm. The average classification accuracy of the proposed approach was found to be high through the cross-validation of the images. A simple and effective method for texture-based weed classification [10] using local pattern operators. The performance of the proposed approach in the classification of weed images was found to be superior when compared to the existing method.

For detecting thistle in sugar beet fields, classification of species was performed using Mahalanobis Distance and Linear Discriminant Analysis [11]. Highest detection accuracy was achieved through the effective selection of features using stepwise linear regression. Finally, the detection results were validated by annotating the images using the trained classifiers. A method for discriminating between weeds based on the combined strategy [12]. The main objective was to achieve appropriate discrimination between the two weed groups under varying conditions of lighting and soil background texture. A novel method of weed recognition based on the invariant moments [13]. The features of the soybean leaf were obtained, and the soybean leaf was recognized using the nearest neighbor classifier. Effective recognition of weed was achieved and rapid, reliable and accurate identification of the weed location were enabled. For processing the leaf images from the inconsistent illumination Radial Basis Function Network (RBFN) classifier was validated for the effective recognition of disease according to the type of deficiencies [14]. The classification accuracy of the deficient leaf was improved.

A smart weed identification technique based on the active shape modeling concept for the morphological identification of the crop and weed [15]. The leaf model was aligned and deformed using automated active shape matching system. The nightshade plants were identified correctly within a short period of time. [16] investigated the usage of machine-learning algorithm for the weed

and crop classification. Testing of the features was performed to find the optimal combination of the significant features that ensures the highest classification rate. The automatic detection of various species with imaging sensors [17]. A sequential classification approach including different Support Vector Machine (SVM) models was chosen for the classification of the weed and crop species. Early identification of the most harmful species was enabled, and optimal classification accuracy was improved.

The accuracy of the wavelet transform method along with SVM and stepwise linear discriminant analysis for the classification of crops and weeds [18]. The stepwise linear discriminant analysis was used for the extraction of the most significant features. Finally, the features were applied for the SVM classification. The classification results were compared with the existing techniques. The overall classification accuracy was improved. An algorithm for detecting the green plant using the hybrid spectral indices. The computation speed of the inter-row weed detection algorithm was higher than the Hough transformation method [19]. In [20] compared and tested the pixel-based and object-based techniques with different classification algorithms, for mapping the weed patches in the wheat fields using multi-spectral satellite image. The pixel based classifications were applied to the wheat fields. Accurate discrimination of the weed patches was achieved.

The utility of SVMs for detecting and mapping the presence of bug weed such as *Solanum mauritianum* within the *Pinus patula* plantations [21]. Higher classification accuracy was achieved and the optimal subset of wavebands for the detection of bug weed was identified using SVM with recursive feature elimination approach. The feasibility of high-resolution imaging techniques for discriminating the sugar beet and thistle and proposed a multispectral camera filter selection protocol [22]. From the simulation results, the improved correct classification rate of the thistles and sugar beets was recognized. An automatic expert identification system was designed based on image segmentation procedures, for the correct identification of plants [23]. The identification performance of the system was improved irrespective of the loss of greenness of the plants. A method for classifying weeds and crops using the morphological analysis. The higher classification rate of the corn and soybean plants and weed was achieved [24].

An advanced technique to enable high herbicide saving and improved crop yield. The usage amount of herbicides was reduced, due to the localized spraying of the infected areas and efficient recognition of weeds [25]. An evolutionary artificial NN (ANN) to minimize the time of classification training and error through the optimization of the neuron parameters [26]. The classification accuracy was improved while avoiding the trial-and-error process of estimating the network inputs according to the histogram data. In [27] proposed an automated weed control system for the effective differentiation of the weeds and crops from the digital image. The classification of the weeds and crops according to the twelve extracted features. The computation cost was reduced and accuracy rate was improved. An herbicide-spraying system was developed in a corn field [28]. The greenness level was computed based on the pixel-by-pixel based comparison of the red, green and blue intensity values of the image. The greenness percent of each image was obtained to generate weed

coverage and patchiness maps. The maps were applied to the Fuzzy logic controller to determine application rate of herbicide in the corn field. In crop and weed discrimination system [29] proposed Random Forest classifier to estimate the crop and weed plants growing in commercial fields if the crop and weed grow close together and overlap between plants. Random Forest classifier to estimate crop and weed certainty at sparse pixel positions based on features extracted from a large overlapping neighborhood. The plant classification system to images from the dataset and performing cross-validation yields an average classification accuracy of 93.8%.

3. PROPOSED WCTATP EXTRACTION METHOD

This section explains about the proposed CTATP Extraction Method for weed identification. To acquire the original images, we used a digital camera (NIKON D90) in this work. Color Images were taken under natural lighting condition from several randomly chosen locations in Agricultural College and Research Institute, Madurai. To explore the effect of the weather and illumination, picture were captured in different conditions. During image collection the camera was located above the scene and focused onto the field at an inclined angle. The sample images are shown in Fig.1. The digital images were stored as 24-bit colour images and saved in RGB color space in the JPG format.



Fig.1. Brinjal crop

The major contributions of the proposed work are,

- Preprocessing techniques are applied to enhance the image, remove the noise.
- Vegetation pixels are extracted from the background under different lighting and environment conditions.
- Wrapping curvelet transformation is applied to the filtered plant image.
- Clear analysis and segmentation of the weed image in the complex background are achieved due to the angular texture pattern extraction at each windowing patch.
- The canny-based edge detection method is used to detect the edges of the weeds from the image.
- Contouring of the edge pixels is performed for the identification of the weed in the plant image.
- Fuzzy rule-based approach is applied to detect the weed patchiness levels.

3.1 PREPROCESSING TECHNIQUES

Pre-processing of the plant image is performed by using the Adaptive Median Filter (AMF), to remove the noise and correct the distortions in the image. The standard median filter cannot distinguish the fine detail from noise. The AMF is designed to overcome the drawbacks of the standard median filter. In the AMF, the size of the window that surrounds each pixel in the image is variable depending on the median value of the pixels in the current 3×3 window. If the median value is an impulse, the size of the window is expanded. Otherwise, further image

processing is done within the current window specifications. The center pixel of the window is estimated to verify whether the center pixel is an impulse or not. The new value of the center pixel in the filtered image is the median value of the pixel in the window if the center pixel is an impulse. The center pixel value is retained in the filtered image, if the center pixel is not an impulse. Thus, the grayscale value of the pixels in the input image and filtered image becomes same, unless the pixel is considered as an impulse. Hence, the AMF removes the impulse noise from the image and reduces distortion in the image.

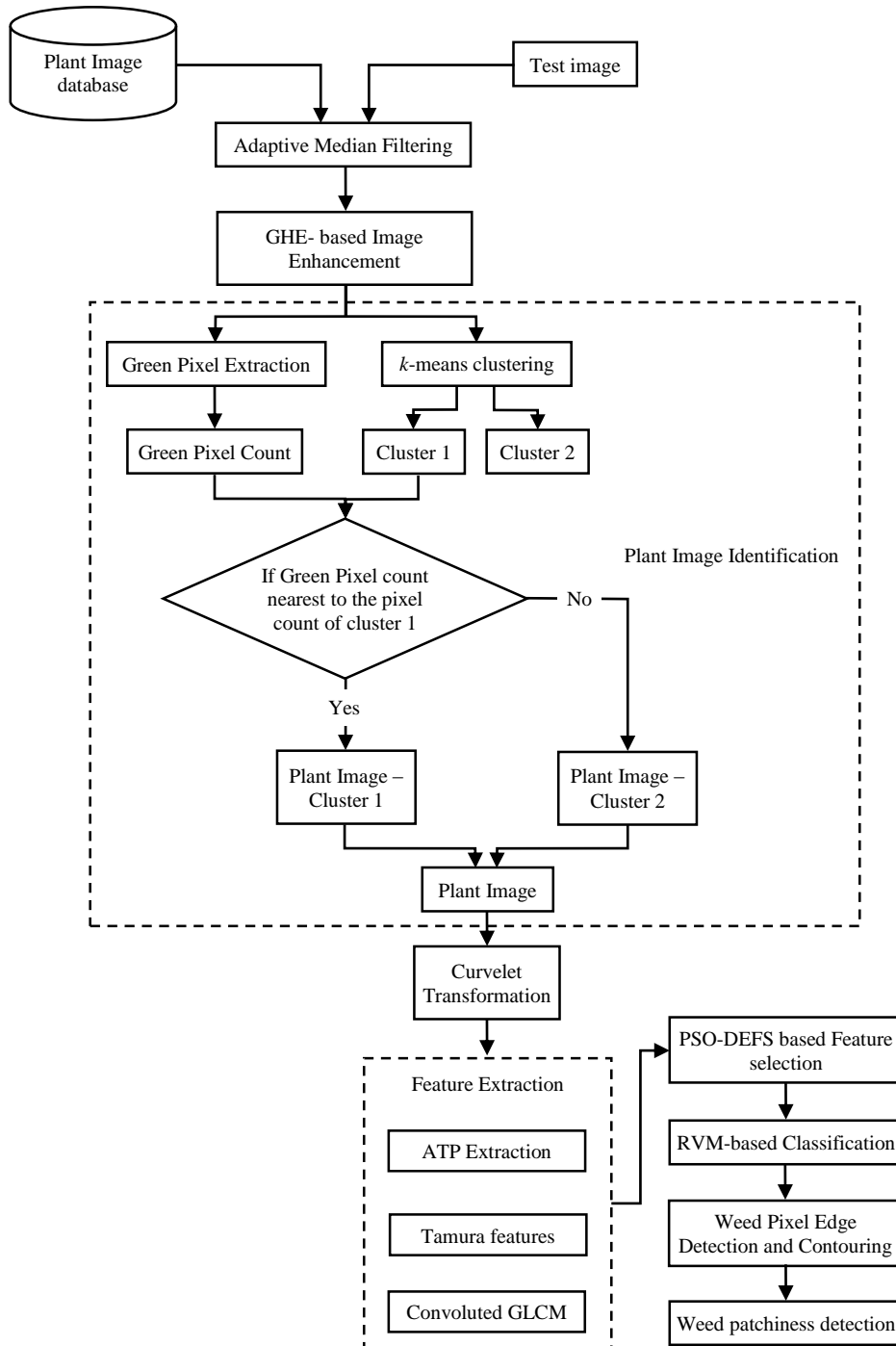


Fig.2. Overall flow diagram of the proposed WCTATP extraction method

The adaptive median filtering approach includes two levels. The first level determines whether the output of the median filter Z_{MED} is an impulse output or not. If the first level fails to find the impulse output, then the second level is executed. The first level is repeated until a median value is found out, or the maximum window size is obtained. The gray level value is obtained from the first level. For each output produced by the algorithm, the window is subsequently moved to the following location in the image. Then, the filtering algorithm is reinitialized again and applied to the pixels in the new location. The median values are updated iteratively using the new pixels, thus reducing the computational overhead.

In the pre-processing stage, Global Histogram Equalization (GHE) was used to improve the quality of the image by lengthening the intensity of the dynamic range using the histogram of the whole image.

Adaptive Mean Filtering Algorithm

Level: 1 Find $A_1 = Z_{MED} - Z_{MIN}$ and $A_2 = Z_{MED} - Z_{MAX}$

If $A_1 > 0$ and $A_2 < 0$, go to Level 2

Else increase the window size

If window size $< S_{max}$, repeat Level 1

Else output Z_{xy}

End If

End If

Level: 2 $B_1 = Z_{xy} - Z_{MIN}$ and $B_2 = Z_{xy} - Z_{MAX}$

If $B_1 > 0$ and $B_2 < 0$

Output Z_{xy}

Else output Z_{MED}

End If

where, ' S_{max} ' denotes the maximum allowed size of S_{xy} and ' S_{xy} ' denotes the size of the neighborhood. Z_{MED} is the median of gray levels in S_{xy} , Z_{MIN} is the minimum gray level value, Z_{MAX} is the maximum gray level value and Z_{xy} is the gray level at coordinates (x, y) . The Fig.3(a) shows the original image of dataset 1 and Fig.2(a) and Fig.2(b) shows the original image of dataset 2. The Fig.4(a) and Fig.4(b) shows the pre-processed images of dataset 1 and dataset 2.

Dataset 1: Brinjal field Images taken from the Agricultural College and Research Institute, Madurai

Dataset 2: Carrot field Images from the existing dataset

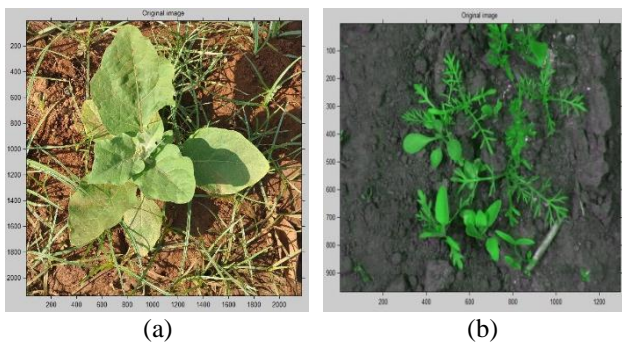


Fig.3 (a) and (b) shows the original images of dataset 1 and dataset 2

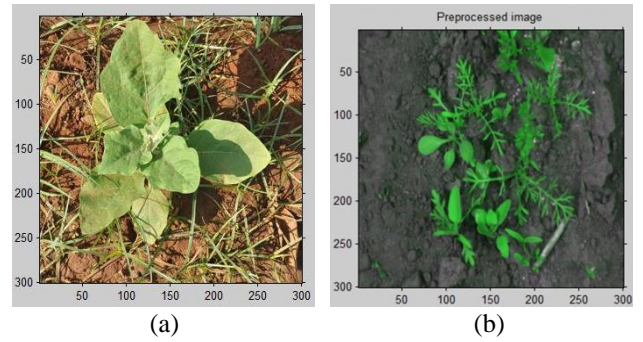


Fig.4. Pre-processed images of dataset 1 and dataset 2

3.2 PLANT IMAGE IDENTIFICATION

The vegetation i.e. crop and other background are identified using the green pixel extraction and k -means clustering process.

3.2.1 Vegetation Segmentation:

After filtering the RGB input image, extraction of the green pixel in the plant image is retrieved for the clear recognition of the plant. Excess Green method (ExG) is used for Green pixel extraction as represented in Eq.(1). Green pixel count is calculated for vegetation extraction. The Fig.5 shows the green pixel extraction process of dataset 1 and dataset 2. The R, G, B represent the Red, Green, Blue channel pixel values.

$$ExG(i, j) = 2 * G(i, j) - R(i, j) - B(i, j) \quad (1)$$

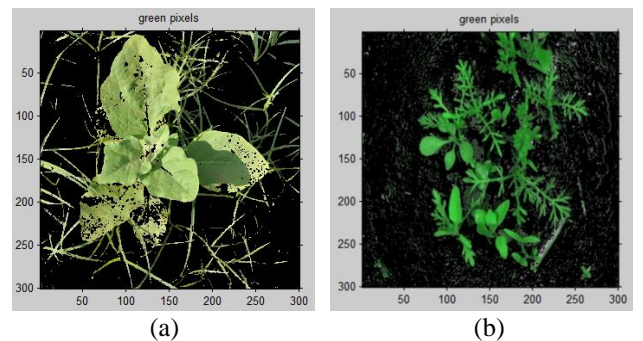


Fig.5(a) and (b) Green Pixel Extraction of dataset 1 and dataset 2

3.2.2 k -means Clustering:

Since the RGB color space does not consider the human perception into account, the CIELAB color space is used in our proposed work to approximate the human vision. The CIELAB color space is used to make accurate color balance corrections or adjust the contrast using the lightness component. The conversion from RGB values to the LAB values involves the transformation of the RGB values to an absolute color space represented as sRGB. Once the colors are converted to sRGB, they are first converted to linear sRGB values and then to the CIE XYZ values. Finally, conversion of colors to the CIE LAB color space is performed using a D65 standard illuminant. Then, the grouping of the pixels into the clusters of dominant colors is performed using a standard k -means clustering algorithm.

The k -means clustering is applied to the filtered image, for separating the soil and plants. It is one of the most frequently used techniques for the automatic partitioning of a data set into ' k ' groups. According to the algorithm, the ' k ' objects are selected as initial cluster centers and the distance between each object and

each cluster center is calculated. The object is assigned to the nearest cluster and the average of all clusters is updated. k -means clustering performs partitioning of data into the k mutually exclusive clusters, and then returns the index of the cluster assigned with each observation. In our proposed work, k -means clustering is used for clustering the filtered image. The Fig.6(a) and Fig.6(b) shows the objects in the Clusters 1 of the dataset 1 and dataset 2. The Fig.7 shows the objects in the cluster 2 of the dataset 1 and dataset 2.

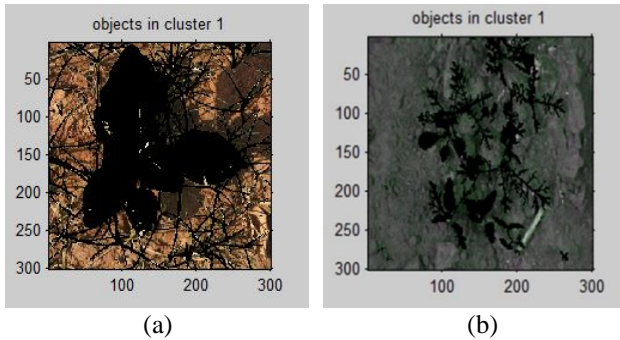


Fig.6 (a) and (b) Objects in cluster 1 of Dataset 1 and Dataset 2

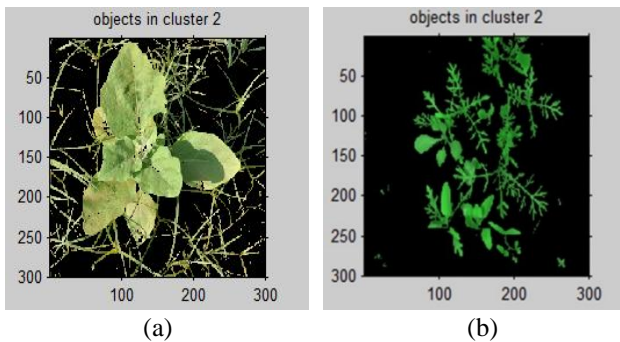


Fig.7 Objects in cluster 2 of dataset 1 and dataset 2

Then, the green pixel count is verified with the pixel count of the clusters. If the green pixel count is nearest to the pixel count of the clusters, then it is considered as the plant image. The plant images of the dataset 1 and dataset 2 are shown in the Fig.8(a) and Fig.8(b).

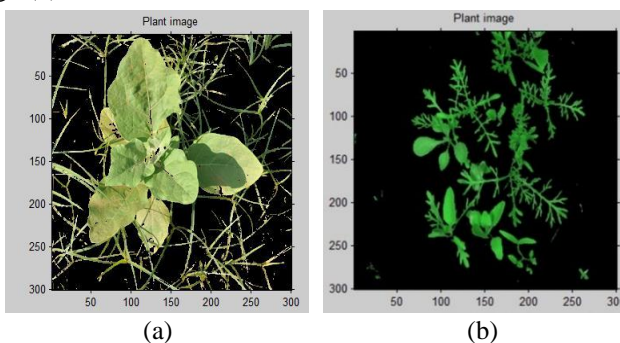


Fig.8(a) and (b) Plant images of dataset 1 and dataset 2

3.3 CURVELET TRANSFORMATION

The main motivation for the development of the curvelet transform is to find a method for representing the edges and singularities along the curves in the efficient way than the existing

methods. The curvelet transform is a multiscale transform, including frame elements that are indexed by the scale and location parameters. The curvelet transform includes directional parameters and curvelet pyramid contains elements with a very high degree of directional specificity. Also, the curvelet transform is based on the certain anisotropic scaling principle. In our work, Wrapping Curvelet Transform is applied to the plant image, to obtain the forward and backward curvelet transformation. Wrapping Curvelet Transform is a multi-scale pyramid that consists of different orientations and positions at a low-frequency level. The wrapping algorithm requires low computation time by using a series of translations and a wraparound technique. The merits of the Fast Fourier Transform (FFT) are used for the multi-resolution discrete curvelet transform in the spectral domain. The image and curvelet at a given scale and orientation are transformed into the Fourier domain, during FFT. A set of curvelet coefficients is obtained by applying inverse FFT to the spectral product, at the completion of the computation process. The curvelet coefficients in the ascending order of the scales and orientations are included in the set. The frequency response of the curvelet is in the form of the trapezoidal wedge. For the inverse Fourier transform, wrapping of the frequency response of the curvelet into a rectangular support is performed. Wrapping of this trapezoidal wedge is done by periodically tiling the spectrum inside the wedge and collecting the rectangular coefficient area in the origin. With the periodic tiling, the rectangular region collects the corresponding fragmented portions of the wedge from the surrounding parallelograms.

The Wrapping Curvelet Transform involves the following steps:

1. Obtain the Fourier Samples by applying the FFT $\hat{F}(n_1, n_2)$, where $-n/2 \leq n_1, n_2 < n/2$.
2. Generate the product for each scale ' m ' and angle ' θ ' $\hat{C}_{m,\theta}[n_1, n_2] \hat{F}[n_1, n_2]$ where ' C ' denotes the Cartesian window
3. Wrap this product about the origin and obtain $\hat{F}_{m,\theta}[n_1, n_2] = W(\hat{C}_{m,\theta} \hat{F})[n_1, n_2]$, where the range of n_1 and n_2 is $0 \leq n_1 < K_{1,m}$ and $0 \leq n_2 < K_{2,m}$. ' θ ' is the range of $(-\pi/4, \pi/4)$.
4. Apply inverse FFT to the $\hat{F}_{m,\theta}$, thus collect the discrete coefficients $D(m, \theta, p)$ where ' p ' is the spatial location parameter.

The number of curvelet decomposition levels for the curvelet transform is determined using the following formula

$$N = \text{Log}_2(\text{Size}(M, 1)) - 2 \quad (2)$$

where, ' N ' is the number of levels and ' M ' is the number of rows. The size of the plant image is 300×300 . By applying the size in the Eq.(2), the number of levels for the curvelet transformation is 6. Hence, six levels of curvelet decomposition are applied to the input image. The Fig.9(a) and Fig.(b) shows the curvelet transformed image of the dataset 1 and dataset 2.

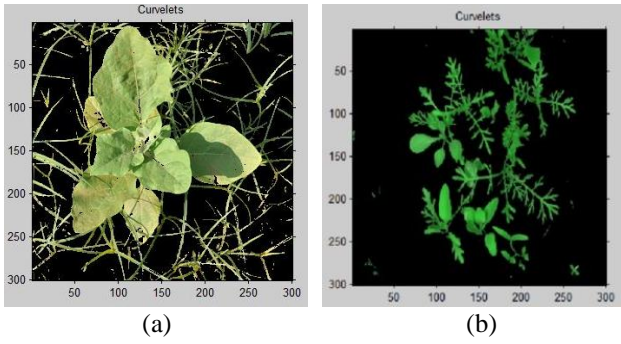


Fig.9 (a) and (b) Curvelet transformed image of dataset 1 and dataset 2

3.4 FEATURE EXTRACTION

Feature extraction is the process of defining a set of features, for the efficient representation of the information for analysis and classification.

In crop and weed classification two very close regions that have differing pixel values will give rise to edges; and these edges are typically curved for crop or weed. As curvelets are good at approximation curved singularities, they are fit for extracting crucial edge-based features from images more efficiently than that compared to wavelet transform.

In our proposed work Wrapping Curvelet Transformation are applied separately for each subband. After applying curvelet transformation the curvelet coefficients have been retrieved from the image. In our crop and weed feature extraction step, in deliberation of computational complexity, all the levels of curvelet coefficients are used for discrimination. In curvelet feature extraction level 2 and level 5 sub-bands coefficients are selected for feature extraction in a 6 levels decomposition of images. The reason for this selection is level 2 coefficients are in ‘finer’ details of an image, they can be used as the texture description of the image, and coefficients in level 5 on the contrary, they are in a ‘coarser’ level, they are fittable for description of the edges in an image. The selection is appropriate since level 2 describe the image in a coarser view and the level 5 coefficients are detail descriptions. The mean value of each color space of sub-band level 2 and level 5 is calculated. In order to improve the feature extraction process, texture feature are used for crop and weed discrimination. After applying curvelet transformation the image was divided into 100 patches of size 30×30 for accurate feature extraction and weed classification. The Fig.9 show the separated patches of the input image of dataset 1 and dataset 2.

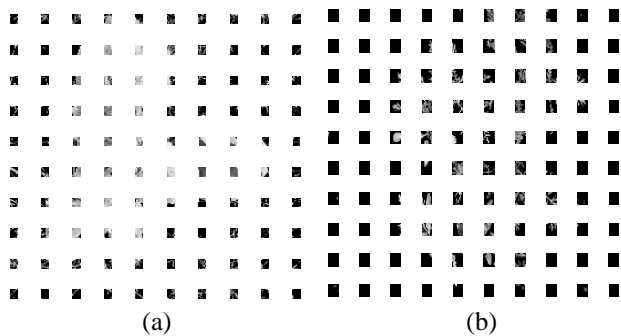


Fig.10. Patch Separation for dataset 1 and dataset 2

3.4.1 Angular Texture Pattern Extraction:

After applying the curvelet transformation, the angular based features are extracted from the transformed image. The main limitations of the Local Binary Patterns (LBP) are the sensitivity of the long histograms to the image rotation, the small spatial area of support, loss of local textural information and sensitivity to noise. Hence, the extraction of angular texture pattern is performed to overcome the limitations of the LBP. In the texture pattern analysis, a novel system of MWP system is presented to predict and analyze the difference in the texture of the image. In the window projection method, the texture pattern is extracted using the enhanced model of the angular texture pattern extraction method.

In the angular texture pattern extraction method, the images are divided into patches, such that each patch contains a 3×3 window. Then, the diagonal pattern is applied. The window is divided into 3×3 cells. The average of diagonal pixels is calculated and replaced with all diagonal pixels. When the average pixel value is greater than or equal to the neighbor pixel value, then the value of ‘1’ is written. Otherwise, the value of ‘0’ is written. Thus, an 8-digit binary number is obtained. Usually, this binary value is converted to decimal for convenience. By counting the number of zeroes and ones, the pattern count of ones placed in left and count of zeroes placed in the right are generated. The histogram related to the frequency of occurrence of each number is computed. The histogram is normalized and all the cells of the normalized histograms are concatenated. Finally, the angular texture pattern feature vector is obtained for the window.

Angular Texture Pattern Extraction Algorithm

Input: Image

Output: Texture pattern image

Divide Image into 3×3 window

Calculate Average of diagonal pixels

For $i = 2:m-1$

For $j = 2:n-1$

$temp = im(i-1:i+1, j-1:j+1, cc);$

$t_s = mean([temp(1) temp(3) temp(7) temp(9) temp(5)]);$

//calculate average of center and diagonal pixels

$temp1(1) = im(i-1, j) > t_s;$

$temp1(2) = im(i-1, j+1) > t_s;$

$temp1(3) = im(i, j+1) > t_s;$

$temp1(4) = im(i, j-1) > t_s;$

$temp1(5) = im(i+1, j+1) > t_s;$

$temp1(6) = im(i+1, j) > t_s;$

$temp1(7) = im(i+1, j-1) > t_s;$

$temp1(8) = im(i, j-1) > t_s;$

$temp1(9) = im(i, j) > t_s;$

Count = 0;

Count1 = 0;

For $i = 1:9$

For $temp(i,:) == 1;$

Count = Count + 1;

Else

Count1 = Count1 + 1;

EndFor

EndFor

EndFor

EndFor

Pattern = [count1 count];

Replace all pixels by the new pattern

Get the texture pattern image

where, ' t_s ' represents the average value of diagonal and center pixel. If the neighbor value of the center pixel is greater than the average value, it is considered as '1' otherwise '0'. In our proposed work, the pattern is extracted from the input image based on the diagonal pixel values. For example in the below 3×3 matrix.

3	4	5
6	7	8
9	10	11

3	4	5
6	7	8
9	10	11

The average of the values 3, 5, 7, 9, 11 is $3 + 5 + 9 + 11 + 7 = 35/5 = 7$.

The original LBP operator labels the pixels in the image by thresholding the neighborhood value of each pixel with the center pixel value and considering the result as a binary number. The binary value 00001111 was generated by the proposed angular texture pattern extraction process. The binary value of this pattern contains four zeros and four ones. Hence, the pattern 45 is generated. Likewise, the patterns are generated.

3.4.2 Tamura Features:

After extraction of the angular texture pattern, the Tamura features are extracted from the image. Textural features corresponding to human visual perception are very useful for optimum feature selection and texture analyzer design. [30] took the approach of devising texture features that correspond to human visual perception. They defined six textural features (coarseness, contrast, directionality, line-likeness, regularity and roughness) and compared them with psychological measurements for human subjects. The Tamura features characterize the low-level statistical properties of the images. The Tamura features are discussed as follows.

3.4.2.1 Coarseness (F_{coa}):

Coarseness is a measure of the size of the texture elements. It provides us with the information about the size of the coarse and fine textures elements. Fine textures have smaller coarse value than the coarse textures.

$$F_{coa} = \frac{2^q}{M^2} \sum_i^M \sum_j^M P(i, j) \quad (3)$$

where, $M \times M$ denotes the size of the image, $P(i, j)$ is the sum of each pixel and ' q ' is the difference of the moving averages.

3.4.2.2 Contrast (F_{con}):

Contrast defines the difference in the intensity value among the neighboring pixels. The image contrast is influenced by the dynamic range of gray levels in the image, polarization of the

distribution of the black and white, sharpness of edges and period of repeating patterns. It could also stand for picture quality in the narrow sense.

$$F_{con} = \frac{\sigma}{\sqrt[4]{\gamma_4}} \quad (4)$$

where,

$$\gamma^4 = \frac{\mu_4}{\sigma^4} \quad (5)$$

Here ' μ_4 ' denotes the fourth moment about the mean ' μ ', and σ^2 denotes the variance.

3.4.2.3 Directionality (F_{dir}):

Directionality measures the total degree of directionality, and also differentiates between the different orientations or patterns.

$$F_{dir} = 1 - N_f \cdot N_p \cdot \sum_p^{N_p} \sum_{Q \in R_p} (Q - Q_p)^2 \cdot H_D(Q) \quad (6)$$

where, ' N_p ' is the number of peaks in the histogram, ' Q ' is the quantized direction code, ' Q_p ' is the p^{th} peak position of the histogram, ' R_p ' is the range of the p^{th} peak between the valleys and ' N_f ' is the normalizing factor.

3.4.2.4 Line-Likeness (F_{lin}):

Line-Likeness is defined as the average coincidence of the edge directions that co-occur at pixels separated by a distance ' D ' along the direction.

$$F_{lin} = \begin{cases} \frac{\sum_{a=0}^{n-1} \sum_{b=0}^{n-1} P_D(a, b) \cos\left[(a-b) \frac{2\pi}{n}\right]}{\sum_{a=0}^{n-1} \sum_{b=0}^{n-1} P_D(a, b)} & \text{if } \sum_{a=0}^{n-1} \sum_{b=0}^{n-1} P_D(a, b) > t \\ 0 & \text{Otherwise} \end{cases} \quad (7)$$

3.4.2.5 Regularity (F_{reg}):

The degree of the irregularity is calculated using the following equation,

$$F_{reg} = 1 - \eta(\sigma_{coa} + \sigma_{con} + \sigma_{dir} + \sigma_{reg}) \quad (8)$$

where ' η ' is the normalizing factor and ' σ ' means the standard deviation of the feature in each sub image of the texture.

3.4.2.6 Roughness (F_{rou}):

Roughness represents the concrete variations in the texture of the image.

$$F_{rou} = F_{coa} + F_{con} \quad (9)$$

In our proposed work, energy, entropy and auto correlation values are calculated additionally as texture features.

3.4.2.7 Energy (F_{EN}):

Energy is the measure of the uniformity in the gray distribution level of the image.

$$F_{EN} = \sum_i \sum_j P^2(i, j) \quad (10)$$

where, ' P ' denotes the probability values for the gray scale pixels ' i ' and ' j '.

3.4.2.8 Entropy (F_H):

Entropy is the measure of the amount of the texture information of an image.

$$F_H = \sum_i \sum_j P(i, j) \log P(i, j) \quad (11)$$

3.4.2.9 Auto-Correlation (F_{AC}):

The auto-correlation is used to measure the degree of similarity of the elements in the image. It decreases quickly and offers a lot of variations, for the images with the low degree of coarseness.

$$F_{AC} = 1 - n_f \left(\frac{kurtosis(con) + kurtosis(dir) + kurtosis(lin) + kurtosis(rou)}{4} \right) + F_{rou} \quad (12)$$

The auto-correlation is computed based on the contrast, directionality, line-linkedness and roughness values.

3.4.3 Convolved GLCM:

One of the most popular signal processing based approaches for texture feature extraction has been the use of Gabor filters. These enable filtering in the frequency and spatial domain. Gabor filter is the most popular tool for feature extraction. It includes the convolution of an image using several multi-orientation filters. It has been proposed that Gabor filters can be used to model the responses of the human visual system. In our proposed work, the image is convoluted along four different orientations (0, 45, 90, and 135). The Gabor filter is used to obtain the clear texture of the image. A transformed space is created for each convolution, and the feature extraction is done in each transformed space. The features vector includes the energy measure of each convoluted image. The Gabor filter is the product of the Gaussian Kernel and the complex sinusoid. The Gaussian curve is represented as,

$$G(x, y, \sigma) = \frac{1}{2\pi\sigma^2} \cdot \exp\left(-\frac{x^2 + y^2}{2\sigma^2}\right) \quad (13)$$

The complex sinusoid is defined as follows,

$$s(x, y, u, \theta, \varphi) = \exp\{j2\pi(x.u\cos\theta + y.usin\theta) + \varphi\} \quad (14)$$

where, ‘ u ’ denotes the spatial frequency, ‘ θ ’ denotes the orientation and ‘ φ ’ represents the phase shift. The complex Gabor function ‘ H ’ is given as,

$$H(x, y, u, \theta, \varphi) = G(x, y, \sigma) \cdot s(x, y, u, \theta, \varphi) \quad (15)$$

The input image $I(x, y)$ is convolved with the Gabor filter ‘ H ’ to produce a set of complex signals ‘ C ’.

$$C(x, y) = I(x, y) \otimes H(x, y, u, \theta, \varphi) \quad (16)$$

The real and imaginary parts of the image are separated as given below,

$$R(x, y) = \text{Re}\{J(x, y)\} \quad (17)$$

$$I(x, y) = \text{Im}\{J(x, y)\} \quad (18)$$

After applying Gabor filter, GLCM features are extracted. Gray Level Co-occurrence Matrix (GLCM) is a statistical method for examining texture features that consider the spatial relationship of pixels, also known as Gray Level Spatial Dependence. In this a GLCM matrix is created by calculating how often a pixel with the intensity value i occurs in a specific spatial relationship to a pixel with the value j . GLCM consists of frequencies at which two pixels are separated by a certain vector occur in the image. GLCM properties by which the distribution in the matrix will depends on the distance and angular or directions like horizontal, vertical, diagonal, anti-diagonal relationship between the pixels. Many statistical features of texture in an

image are based on the co-occurrence matrix representing the second order of gray levels pixels relationship in an image. Various statistical and information theoretic properties of the co-occurrence matrices can serve as textural features and the limitation with these features are expensive to compute, and they were not very efficient for image classification and retrieval. In [31] proposed 28 kinds of textural features each extracted from the Gray Level Co-occurrence Matrix.

GLCM features are extracted from the Gabor filtered image. GLCM is defined as a square matrix that defines the spatial distribution of the gray levels in the image. The GLCM is used to compute a set of scalar quantities that characterize the different aspects of the texture in the image. It defines about the linear relationship between the reference pixel ‘ i ’ and neighboring pixel ‘ j ’ located within the area of interest. Each element (a, b) is the number of co-occurrences of the pixels. The pixels are located at a distance ‘ D ’ with respect to each other. The GLCM is computed by using the following equation,

$$C_{a,b,\varphi} = \sum_{i=1}^M \sum_{j=1}^M \begin{cases} 1, & \text{if } I(i, j) = a \text{ and } I(i + \varphi_i, j + \varphi_j) = b \\ 0 & \text{Otherwise} \end{cases} \quad (19)$$

where, ‘ φ_i ’ and ‘ φ_j ’ denote the relative orientations of the pixels ‘ i ’ and ‘ j ’. ‘ a ’ represents the gray level of the pixels (i, j) and ‘ b ’ represents the gray level of the pixels ($i + \varphi_i, j + \varphi_j$). During the analysis of statistical texture, computing of the texture features is performed from the statistical distribution of the observed combinations of intensities at specified positions in the image. GLCM method is a method of extracting the second order statistical texture features. The number of rows and columns in the GLCM matrix is equal to the number of gray levels ‘ G ’ in the image. The pixels are separated by the distances δ_x and δ_y within a given neighborhood. The matrix element $P(i, j | \delta_x, \delta_y)$ is the relative frequency with which the pixels are separated. The gray levels of the pixels are ‘ i ’ and ‘ j ’. The matrix element $P(i, j | d, \theta)$ includes the second order statistical probability values for the difference between the gray levels at a particular displacement distance ‘ d ’ and at an angle ‘ θ ’. The GLCM features are described below,

$$F_{ENG} = \sum_{i=1}^N \sum_{j=1}^N \{S(i, j)^2\} \quad (20)$$

$$F_{CON} = \sum_{i=1}^N \sum_{j=1}^N [(i - j)^2 * S(i, j)] \quad (21)$$

$$F_{CORR} = \frac{1}{\sigma^2} \left\{ \left(\sum_i \sum_j i \cdot j \cdot S(i, j) \right) - \mu^2 \right\} \quad (22)$$

$$F_{VAR} = \sum_{i=1}^N \sum_{j=1}^N (i - \mu)^2 S(i, j) \quad (23)$$

$$F_{HOM} = \sum_{i=1}^N \sum_{j=1}^N \frac{S(i, j)}{1 + (i - j)^2} \quad (24)$$

$$F_{AVG} = \sum_{i=2}^{2N} i \cdot P_{xy}(i) \quad (25)$$

$$P_{xy}(i + j) = \sum_{i=1}^N \sum_{j=1}^N S(i, j) \quad (26)$$

$$F_{SE} = - \sum_{i=2}^{2N} f_{se}(i) \quad (27)$$

$$f_{se}(i) = P_{xy}(i) \log_e P_{xy}(i) \quad (28)$$

$$F_{SV} = \sum_{i=2}^{2N} f_{sv}(i) \quad (29)$$

$$f_{sv}(i) = (i - F_{ENT})^2 \cdot P_{xy}(i) \quad (30)$$

$$F_{ENT} = - \sum_{i=1}^N \sum_{j=1}^N S(i, j) \cdot \log_e S(i, j) \quad (31)$$

$$P_x(i) = \sum_{j=1}^N S(i, j) \quad (32)$$

$$P_y(j) = \sum_{i=1}^N S(i, j) \quad (33)$$

$$h_x(i) = P_x(i) \cdot \log_e P_x(i) \quad (34)$$

$$h_y(j) = P_y(j) \cdot \log_e P_y(j) \quad (35)$$

$$h_{xy1}(i, j) = S(i, j) \cdot \log[P_x(i) \cdot P_y(j)] \quad (36)$$

$$h_{xy2}(i, j) = P_x(i) \cdot P_y(j) \cdot \log[P_x(i) \cdot P_y(j)] \quad (37)$$

$$H_{xy} = F_{ENT} \quad (38)$$

$$H_X = - \sum_{i=1}^N h_x(i) \quad (39)$$

$$H_Y = - \sum_{j=1}^N h_y(j) \quad (40)$$

$$H_{XY1} = - \sum_{i=1}^N \sum_{j=1}^N h_{xy1}(i, j) \quad (41)$$

$$H_{XY2} = - \sum_{i=1}^N \sum_{j=1}^N h_{xy2}(i, j) \quad (42)$$

$$F_{INF1} = \frac{H_{XY} - H_{XY1}}{\max(H_X, H_Y)} \quad (43)$$

$$F_{INF2} = \sqrt{1 - \exp\{-2(H_{XY2} - H_{XY})\}} \quad (44)$$

$$F_{IDM} = \sum_{i,j} \frac{P(i, j)}{1 + |i - j|} \quad (45)$$

F_{ENG} represents of the homogeneous energy measure of the image texture. This energy value is high for the homogeneous images. F_{CON} is a measure of the texture contrast. This value is high for the high contrast images. F_{CORR} represents the measure of correlation between the pixels located at the specific positions relative to each other. F_{VAR} represents the measure of variance in the image texture. The variance value is high, when the values deviate largely from the average value. F_{HOM} is a measure of the homogeneity value of the image texture. F_{AVG} is the sum average value proportional to the sum of the left-side diagonal elements of the GLCM. F_{SE} is the sum entropy and is a measure of the randomness of the image. F_{SV} is the sum variance and is a measure of the deviation from the entropy. F_{ENT} denotes the entropy of the image. The entropy value is high for non-homogeneous image. F_{INF1} and F_{INF2} denote the information measures of correlation features 1 and 2. F_{IDM} denotes the Inverse Difference Moment of the image texture. For a highly textured image, the value of IDM is 0 and the value is 1 for the untextured image. One mean value is obtained for each patch of the plant image, from the angular texture pattern extraction process. The Tamura features outputs 6 features and convoluted GLCM outputs 12 features. Totally, 21 features are obtained.

The curvelet transformation provides 3 mean values. Three values are obtained from the ATP extraction process. The Tamura features outputs 6 features and convoluted GLCM outputs 12 features. Totally, 24 features are obtained. In the feature extraction process, 1×21 features are obtained for each patch of the image. Totally $3 + (100 \times 21)$ features are extracted for the whole image for efficient weed classification for spot spraying herbicide application.

3.5 FEATURE SELECTION

Feature selection is the process of selecting a subset from a set of original features. Feature selection is the dimensionality reduction technique. The feature selection technique is used to remove the noisy features to improve the quality of the image and efficient classification. The feature selection is performed by using PSO-combined Differential Evolution Feature Selection (DEFS) approach. This is done to select a minimum set of features to achieve better feature selection performance. The Table.1 Shows the list of features retrieved from the plant image.

Table.1. Input Feature list for PSO

Sl. No.	Features
1	Curvelet mean value of red channel
2	Curvelet mean value of green channel
3	Curvelet mean value of blue channel
4	Angular texture pattern mean value of red channel
5	Angular texture pattern mean value of green channel
6	Angular texture pattern mean value of blue channel
7	GLCM - Auto correlation
8	GLCM - Contrast
9	GLCM - Correlation matlab
10	GLCM - Correlation p
11	GLCM - Cluster prominence
12	GLCM - Cluster shade
13	GLCM - Dissimilarity
14	GLCM - Energy
15	GLCM - Entropy
16	GLCM - Homogeneity Matlab
17	GLCM - Homogeneity P
18	GLCM - Maximum probability
19	Tamura - Coarseness
20	Tamura - Contrast
21	Tamura - Directionality
22	Tamura - Entropy
23	Tamura - Energy
24	Tamura - Auto correlation

3.5.1 PSO-Combined DEFS Approach:

In the PSO technique, a population called as a swarm of candidate solutions is encoded as particles in the search space. PSO begins with the random initialization of the population. The whole swarm moves in the search space, for searching the best solution.

Searching of the best solution is performed by updating the position of each particle. During the movement of the swarm, a vector $X_i = (X_{i1}, X_{i2}, \dots, X_{id})$ represents the current position of the particle 'i'. $V_i = (V_{i1}, V_{i2}, \dots, V_{id})$ represents the velocity of the particle in the range of $[-v_{max}, v_{max}]$. The best previous position of a particle is denoted as personal best P_{best} . The global best position obtained by the population is denoted as G_{best} . The PSO searches for the optimal solution by updating the velocity and position of each particle, based on the P_{best} and G_{best} . The PSO reduces 22 features to 17 features.

Table.2. Features obtained using PSO

Sl. No.	Features
1	Curvelet mean value of red channel
2	Curvelet mean value of green channel
3	Curvelet mean value of blue channel
4	Angular texture pattern mean value of red channel
5	Angular texture pattern mean value of green channel
6	Angular texture pattern mean value of blue channel
7	GLCM - Auto correlation
8	GLCM - Correlation matlab
9	GLCM - Correlation p
10	GLCM - Cluster prominence
11	GLCM - Cluster shade
12	GLCM - Dissimilarity
13	GLCM - Energy
14	GLCM - Entropy
15	GLCM - Homogeneity P
16	GLCM - Maximum probability
17	Tamura - Coarseness
18	Tamura - Contrast
19	Tamura - Directionality
20	Tamura - Entropy

Differential Evolution (DE) is a parallel and direct search method that provides near-optimal solutions for the fitness function of the optimization problem. The parameters of the search space are encoded in the form of strings. A collection of the strings is termed as population denoted as 'P'. It is a collection of predefined number 'N' of parameter vectors $x_{j,G} = [x_{1,j,G}, x_{2,j,G}, \dots, x_{D,j,G}]$, where, $j = 1, 2, \dots, N$ for each generation 'G'. 'D' represents the number of real parameters. The value of 'N' does not change during the minimization process. Random selection of the initial vector population that represents the different points in the search space is performed. The fitness function is associated with each string that represents the degree of the wellness of the string. During the mutation operation, the weighted difference between the two population vectors is added to a third vector, to generate new parameter vectors. Then, the crossover operation is performed by mixing the mutated vector's parameters with the parameters of the target vector, to produce the trial vector. During the selection process, the target vector is replaced by the trial vector in the subsequent generation, if the trial vector produces a lower cost function value than the target vector. The process of

selection, crossover and mutation continues for a fixed number of generations or until a termination condition is satisfied. The DEFS reduces 17 features to 15 features. The Fig.13(a) and Fig.13(b) shows the PSO output for the images in dataset 1 and dataset 2.

PSO combined DEFS Algorithm

Input: Feature Values, Number of parameters to be optimized, maximum number of iteration

Step 1: Randomly initialize position, No of Iterations, Velocity of Each Particle

Step 2: While $i < \text{maxiteration}$

Step 3: Evaluate Fitness for each particle

Step 4: $\text{Val} = \sum_{i=1}^n \text{skewness}(i, j) / \text{skewness}(i+1, j);$

Step 5: pbest = val;

Step 6: for $i = 1$ to popsize do

Step 7: update P_{best} of particle

Step 8: update G_{best} of particle

Step 9: for $i = 1$ to PopulationSize do

Step 10: for $d = 1$ to Dimensionality do

Step 11: update the velocity of particle i

Step 12: update the position of particle i

Step 13: end for

Step 14: end for

Step 15: end for

Step 16: end while

The fitness value for each particle is evaluated based on the skewness of the feature values. The personal best solution of the particle is determined from the fitness value. The personal best solution and global best solution of the particle are updated. Finally, the position and velocity of the particle are updated. The Table.3 shows the number of features obtained from the DEFS approach.

Table.3. Features obtained from the DEFS approach

Sl. No.	Features
1	Curvelet mean value of red channel
2	Curvelet mean value of green channel
3	Angular texture pattern mean value of red channel
4	Angular texture pattern mean value of green channel
5	Angular texture pattern mean value of blue channel
6	GLCM - Correlation matlab
7	GLCM - Correlation p
8	GLCM - Cluster prominence
9	GLCM - Cluster shade
10	GLCM - Energy
11	GLCM - Homogeneity P
12	GLCM - Maximum probability
13	Tamura - Coarseness

14	Tamura - Contrast
15	Tamura – Entropy

After the selection of features, the classification of the image is performed by using the RVM based classification.

3.6 RVM BASED CLASSIFICATION

For a crop and weed discrimination system is divided into two stages: a training stage and a classification stage. In the training stage, a set of known crop with weed (labeled data) are used to create a representative feature-set or template. In the classification stage, an unknown crop with weed image is matched against the previously stored database by comparing the features. Curvelet based feature extraction takes the preprocessed crop with weed images as input. The RVM classifier is used for classification task.

The advantages of RVM are (i) RVM classifier requires lesser amount of relevance vector than the SVM (ii) Testing time of the RVM is lower than the SVM and the design complexity (iii) cost of the RVM are also lower than the SVM.

The classification of the selected features in the plant image is performed using the RVM based classification technique. Selected features are learned and passed through the RVM classifier for finding the weed. RVM is a Bayesian regularization framework to obtain the solution for binary classification. The training time of the RVM shows the quadratic increase with the increase in the number of data points. The likelihood is defined as,

$$P(c/w) = \prod_{i=1}^n \sigma\{y(x_i)\}^{c_i} [1 - \sigma\{y(x_i)\}]^{1-c_i} \quad (46)$$

where, $X = (x_1, x_2, \dots, x_n)$ is the training data having class labels $C = (c_1, c_2, \dots, c_n)$ with $c_i \in (-1,1)$. $\sigma(y)$ is the logistic sigmoid function defined as,

$$\sigma(y(x)) = \frac{1}{1 + \exp(-y(x))} \quad (47)$$

An iterative method is used to obtain $P(c/w)$. Let α_i^* denotes the maximum aposteriori estimate of the hyper parameter α . The maximum aposteriori estimate of the weights (W_m) is obtained by maximizing the following objective function,

$$f(w_1, w_2, \dots, w_n) = \sum_{i=1}^n \log p(c_i/w_i) + \sum_{i=1}^n \log p(w_i/\alpha_i^*) \quad (48)$$

In the resulting solution, the gradient of the objective function with respect to weight is calculated. The training data having non-zero coefficients w_i called as relevance vectors contribute to the decision function. The RVM classification is performed to reduce the dimensionality of feature set and correct grouping of classified feature set vectors by using a small number of features. The crop region in the plant image is classified as 1. After identifying the crop region, remaining blocks are extracted from the plant image. The Fig.11(a) and Fig.11(b) shows the RVM classified crop images of dataset 1 and dataset 2. The Fig.12(a) and Fig.12(b) shows the extraction of the remaining regions from the plant image, after identifying the crop blocks.

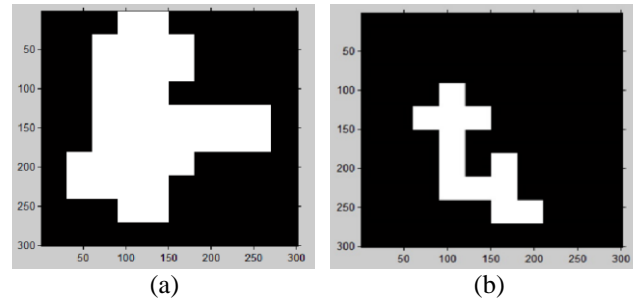


Fig.11 (a) and (b) RVM classified crop images of dataset 1 and dataset 2

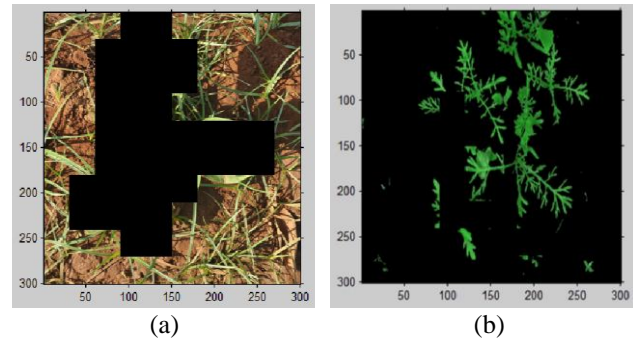


Fig.12 (a) and (b) Extraction of the remaining regions from the plant images of dataset 1 and dataset 2

3.7 WEED EDGE DETECTION AND CONTOURING

The canny based edge detection method is used to detect the edges of the weeds from the image. Initially, the canny edge detector performs smoothing of the image to filter the noise in the original image, before locating and detecting the edges. The Gaussian filter is used in the Canny algorithm, since it is computed using a simple mask. Once the suitable mask is decided, Gaussian smoothing is performed using the standard convolution techniques. The convolution mask is made to slide over the image, to manipulate the square of pixels. During the increase in the Gaussian Width, there is a slight increase in the localization error in the detected edges. After performing the image smoothing and noise removal, the edge strength is found out by considering the gradient value of the image. The Sobel operator performs the two-dimensional spatial gradient measurement. Then, the approximate absolute gradient magnitude at each point is found. The Sobel operator utilizes a pair of 3x3 convolution masks, to estimate the gradient along the X-direction and Y-direction. The magnitude of the gradient is approximated using the formula,

$$|G| = |G_x| + |G_y| \quad (49)$$

The edge direction is computed using the gradient values along the 'X' and 'Y' directions. If G_x is equal to zero, the edge direction is equal to 0 or 90 degree, based on the value of G_y . If G_y is equal to zero, the edge direction is equal to 0 degree. The edge direction is computed by using the following equation,

$$\theta = \tan^{-1} \frac{G_y}{G_x} \quad (50)$$

Once the edge direction is computed, the edge direction is related to the tracing direction in the image. Then, non-maximum

suppression is used to trace along the edges and suppress the pixel value that is not considered as edge pixels. A thin line is formed in the output image. Then, hysteresis thresholding is used for detecting the real edges using the maximum and minimum threshold values. The edges having the intensity gradient value more than the maximum threshold value are considered as the real edges. The gradient value of the edges lying below the minimum threshold value is detected as non-edges and discarded. The edges lying between the thresholds are classified as edges or non-edges based on their connectivity. The Fig.13(a) and Fig.13(b) shows the weed edge detection for dataset 1 and dataset 2.

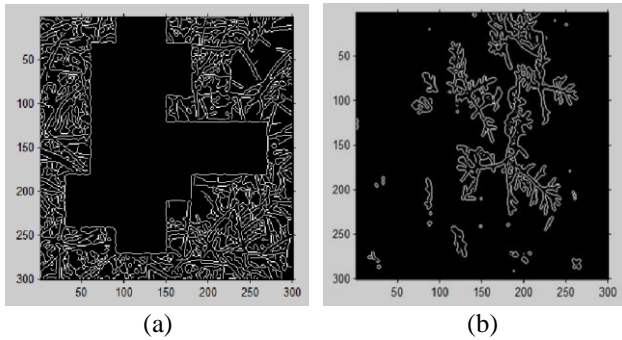


Fig.13 (a) and (b) Weed edge detection for dataset 1 & dataset 2

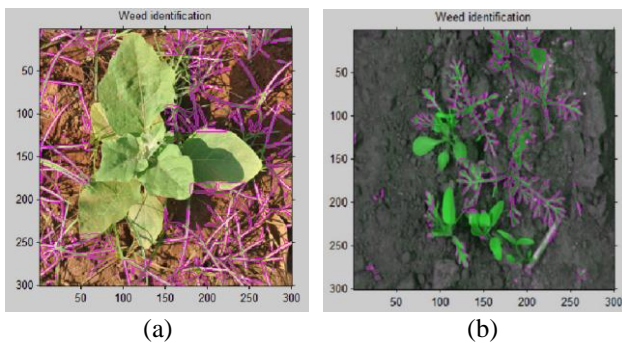


Fig.14 (a) and (b) Weed identification for dataset 1 & dataset 2

After detecting the edges, the contour is drawn over the edges. Then, the edge pixels are colored for the identification of weed in the plant image. The Fig.17(a) and Fig.17(b) shows the weed identification for dataset 1 and dataset 2.

3.8 FUZZY RULE-BASED WEED PATCHINESS DETECTION

Fuzzy rule-based approach is used for detecting the weed patchiness level [23]. The Fuzzy Logic Toolbox of MATLAB is used to develop the fuzzy logic algorithm. Fuzzy logic control is based on the mathematical concept called as ‘membership function’. The weed patchiness count is applied as an input to the toolbox and the level of the weed patchiness is obtained as the output. There are three levels of the weed patchiness are high, medium and low. If the weed patchiness count lies within the specific range, it is classified as ‘medium’ and ‘low’ levels. Otherwise, it is considered as ‘high’ level.

If the weed patchiness value lies between 6000 and 8000, it is considered as ‘Low’ level. If the patchiness lies between 8000 and 9000, it is considered as ‘Medium’ level. If the patchiness lies beyond 9000, it is considered as ‘high’ level.

4. PERFORMANCE ANALYSIS

This section presents the performance analysis results of the proposed WCTATP approach. In the proposed work, the angular texture pattern of the image is extracted, and selection of the optimal features is performed using the PSO-based DEFS approach. Classification of the weed region is done using RVM based approach. With the extraction of the angular texture pattern at each windowing patch, clear analysis of the plant image in the complex background is achieved. In our work, Dataset 1 includes the Real-time plant image obtained from the Agricultural College and Research Institute, Madurai. Dataset 1 includes 500 images. The dataset 2 is a benchmark dataset comprising 60 images, for crop/weed discrimination [25]. This dataset includes the field images in the top-down view acquired using the autonomous field robot in an organic carrot farm. A set of 560 images is used for training, and a set of 500 images is used for testing. The performance of the proposed approach is evaluated using a set of 150 images. The metrics used for evaluating the performance of the proposed approach is Accuracy.

Accuracy

Accuracy is defined as the measure of the correctly classification results of the weeds in the plant image. Sensitivity and Specificity are the most important measures to evaluate the performance of the RVM classifier. RVM classifier shows higher sensitivity and specificity value for the input plant images. Sensitivity is a true positive measure indicating the correct classification rate of the weeds. Specificity is a measure of true negative classifications that denotes the incorrect classification of the weeds.

$$\text{Accuracy} = \frac{N_{TP} + N_{TN}}{N_{TP} + N_{TN} + N_{FP} + N_{FN}} \quad (51)$$

where, N_{TP} is the true positive measurement, N_{TN} is the true negative measurement, N_{FP} is the false positive measurement (portion of the image incorrectly classified as weed), and N_{FN} is the false negative measurement (portion of the image incorrectly classified as not a weed).

Table.4. Comparative analysis of Accuracy of the proposed approach

Number of Images	Accuracy (%)
1	0.9848
2	0.985
3	0.9851
4	0.9843
5	0.9841
6	0.9841
7	0.9838
8	0.9838
9	0.9839
10	0.984
11	0.9839
12	0.9838

13	0.9836
14	0.9835
15	0.9833
16	0.9833
17	0.9833
18	0.9832
19	0.9832
20	0.9832
21	0.9832
22	0.9833
23	0.9834
24	0.9834
25	0.9835
26	0.9836
27	0.9836
28	0.9835
29	0.9834
30	0.9834
31	0.9834
32	0.9835
33	0.9834
34	0.9833
35	0.9832

The accuracy level of the proposed method is compared with the accuracy levels of the existing techniques such as SVM approach for classification of crops and weeds from digital image [10] and SVM based Crop/weed classification in maize fields [26].

Table.5. Comparative analysis of accuracy of the proposed and existing techniques

Methods	Accuracy (%)
SVM based Crop/weed classification in maize fields	93.1
SVM approach for classification of crops and weeds from digital image	97.3
Proposed CTATP Extraction Method	98.3

The overall accuracy of the proposed approach is 98.3 %, which is relatively higher than the existing techniques. Hence, the proposed approach is found to be efficient than the existing techniques.

5. CONCLUSION AND FUTURE WORK

The conclusion and future scope of the proposed work are discussed in this section. A novel WCTATP extraction method for weed identification is proposed in this paper. For the pre-processing operation, AMF is used to filter the impulse noise from the plant image and perform smoothing of the image for the clear analysis of textures in the image. Green pixel extraction is performed to obtain the green pixel count from the filtered image.

k -means clustering is applied to the filtered image, to cluster the soil and plants. Then, the green pixel count is verified with the pixel count of the clusters. If the green pixel count is nearest to the pixel count of the clusters, then it is considered as the plant image. Curvelet transformation is applied to the plant image. After applying the curvelet transformation, the angular based features are extracted from the transformed image. Feature extraction is performed to extract the angular texture pattern of the plant image. The Tamura features are extracted from the image, Gabor filter with four orientations is applied to the image and GLCM features are extracted from the Gabor filtered image. PSO-based DEFS is applied to select the optimal features. Then, the selected features are classified using a RVM based classifier to find out the weed. Canny based Edge detection and contouring is performed based on the classified to identify the weed. Fuzzy rule-based approach is used for detecting the low, medium and high levels of the weed patchiness. Clear analysis and segmentation of the plant image in the complex background are achieved due to the angular texture pattern extraction at each windowing patch. The proposed approach achieves better performance in terms of Accuracy. The accuracy of the proposed approach is higher than the existing SVM-based approaches. In our future work, application amount of the herbicides in the weeded area is determined based on the Fuzzy-rule based weed patchiness estimation result.

REFERENCES

- [1] A. Tellaeché, G. Pajares, X.P. Burgos-Artizzu and A. Ribeiro, "A Computer Vision Approach for Weeds Identification through Support Vector Machines", *Applied Soft Computing*, Vol. 11, No. 1, pp. 908-915, 2011.
- [2] A.-G. Manh, G. Rabatel, L. Assemat and M.-J. Aldon, "AE-Automation and Emerging Technologies: Weed Leaf Image Segmentation by Deformable Templates", *Journal of Agricultural Engineering Research*, Vol. 80, No. 2, pp. 139-146, 2001.
- [3] J.B. Vioix, J.P. Douzals, F. Truchetet, L. Assemat and J.P. Guillemin, "Spatial and Spectral Method for Weeds Detection and Localization", *EURASIP Journal on Applied Signal Processing*, Vol. 7, No. 1, pp. 679-685, 2002.
- [4] V. Leemans and M.-F. Destain, "Application of the Hough Transform for Seed Row Location using Machine Vision", *Biosystems Engineering*, Vol. 94, No. 3, pp. 325-336, 2006.
- [5] J.A. Marchant, "Tracking of Row Structure in Three Crops using Image Analysis", *Computers and Electronics in Agriculture*, Vol. 15, No. 2, pp. 161-179, 1996.
- [6] Amal M. Al Gindi, Tawfik A. Attiatalla and Moustafa M. Sami, "A Comparative Study for comparing Two Feature Extraction Methods and Two Classifiers in Classification of Early-stage Lung Cancer Diagnosis of Chest X-ray Images", *Journal of American Science*, Vol. 10, No. 6, pp. 13-22, 2014.
- [7] J. Chaki, R. Parekh, and S. Bhattacharya, "Plant Leaf Recognition using Texture and Shape Features with Neural Classifiers", *Pattern Recognition Letters*, Vol. 58, No. 1, pp. 61-68, 2015.
- [8] S. Haug, A. Michaels, P. Biber and J. Ostermann, "Plant Classification System for Crop/Weed Discrimination without Segmentation", *Proceedings of IEEE Winter*

- Conference on Applications of Computer Vision*, pp. 1142-1149, 2014.
- [9] Wu LanLan and Wen YouXian, "Weed/corn Seedling Recognition by Support Vector Machine using Texture Features", *African Journal of Agricultural Research*, Vol. 4, No. 9, pp. 840-846, 2009.
- [10] F. Ahmed, H. Kabir, S.A. Bhuyan, H. Bari and E. Hossain, "Automated Weed Classification with Local Pattern-based Texture Descriptors", *The International Arab Journal of Information Technology*, Vol. 11, No. 1, pp. 87-94, 2014.
- [11] W. Kazmi, F.J. Garcia-Ruiz, J. Nielsen, J. Rasmussen and H.J. Andersen, "Detecting Creeping Thistle in Sugar Beet Fields using Vegetation Indices", *Computers and Electronics in Agriculture*, Vol. 112, pp. 10-19, 2015.
- [12] P.J. Herrera, J. Dorado and Á. Ribeiro, "A New combined Strategy for Discrimination between Types of Weed", *ROBOT2013: First Iberian Robotics Conference*, pp. 469-480, 2014.
- [13] Z. Bo, W.H. Hua, L.S. Jun, M.W. Hua and Z.X. Chao, "Research on Weed Recognition method based on Invariant Moments", *Proceedings of 11th World Congress on Intelligent Control and Automation*, pp. 2167-2169, 2014.
- [14] N.M. Tahir, S.R.M.S. Baki, M.A. Hairuddin and N.D.K. Ashar, "Classification of *Elaeis Guineensis* disease-leaf under Uncontrolled Illumination using RBF Network", *Proceedings of IEEE International Conference on Control System, Computing and Engineering*, pp. 617-621, 2014.
- [15] K.C. Swain, M. Nørremark, R.N. Jørgensen, H.S. Midtby and O. Green, "Weed Identification using an Automated Active Shape Matching (AASM) Technique", *Biosystems Engineering*, Vol. 110, No. 4, pp. 450-457, 2011.
- [16] F. Ahmed, H. A. Al-Mamun, A. H. Bari, E. Hossain, and P. Kwan, "Classification of Crops and Weeds from Digital Images: A Support Vector Machine Approach", *Crop Protection*, Vol. 40, pp. 98-104, 2012.
- [17] T. Rumpf, C. Römer, M. Weis, M. Sökefeld, R. Gerhards and L. Plümer, "Sequential support vector machine classification for small-grain weed species discrimination with special regard to *Cirsium arvense* and *Galium aparine*", *Computers and Electronics in Agriculture*, Vol. 80, pp. 89-96, 2012.
- [18] M.H. Siddiqi, S.-W. Lee and A.M. Khan, "Weed Image Classification using Wavelet Transform, Stepwise Linear Discriminant Analysis, and Support Vector Machines for an Automatic Spray Control System", *Journal of Information Science and Engineering*, Vol. 30, No. 4, pp. 1227-1244, 2014.
- [19] H. Liu, S.H. Lee and C. Saunders, "Development of a Machine Vision System for Weed Detection During both of Off-Season and In-Season in Broadacre No-Tillage Cropping Lands", *American Journal of Agricultural and Biological Sciences*, Vol. 9, No. 2, pp. 174-193, 2014.
- [20] I.L. Castillejo-González, J.M. Peña-Barragán, M. Jurado-Expósito, F.J. Mesas-Carrascosa and F. López-Granados, "Evaluation of Pixel-and Object-based approaches for Mapping Wild Oat (*Avena Sterilis*) Weed patches in Wheat fields using QuickBird Imagery for Site-Specific Management", *European Journal of Agronomy*, Vol. 59, pp. 57-66, 2014.
- [21] J.T. Atkinson, R. Ismail and M. Robertson, "Mapping Bugweed (*Solanum Mauritanium*) Infestations in Pinus Patula Plantations using Hyperspectral Imagery and Support Vector Machines", *IEEE Journal of Selected Topics in Applied Earth Observations and Remote Sensing*, Vol. 7, No. 1, pp. 17-28, 2014.
- [22] F.J. Garcia-Ruiz, D. Wulfsohn and J. Rasmussen, "Sugar Beet (*Beta vulgaris* L.) and Thistle (*Cirsium arvensis* L.) Discrimination based on Field Spectral Data", *Biosystems Engineering*, Vol. 139, pp. 1-15, 2015.
- [23] M. Montalvo, J.M. Guerrero, J. Romeo, L. Emmi, M. Guijarro and G. Pajares, "Automatic Expert System for Weeds/Crops Identification in Images from Maize Fields", *Expert Systems with Applications*, Vol. 40, No. 1, pp. 75-82, 2013.
- [24] F.-M. De Rainville, A. Durand, F.-A. Fortin, K. Tanguy, X. Maldague, B. Panneton and M.-J. Simard, "Bayesian Classification and Unsupervised Learning for Isolating Weeds in Row Crops", *Pattern Analysis and Applications*, Vol. 17, No. 2, pp. 401-414, 2014.
- [25] A. Tannouche, K. Sbai, Y. Ounejjar and A. Rahmani, "A Real Time Efficient Management of Onions Weeds based on a Multilayer Perceptron Neural Networks Technique", *International Journal of Farming and Allied Sciences*, Vol. 4, No. 2, pp. 161-166, 2015.
- [26] A.M. Tobal and S.A. Mokhtar, "Weeds Identification using Evolutionary Artificial Intelligence Algorithm", *Journal of Computer Science*, Vol. 10, No. 8, pp. 1355-1361, 2014.
- [27] Md Mursalin and Md Mesbah-UI-Awal, "Towards Classification of Weeds through Digital Image", *Proceedings of Fourth International Conference on Advanced Computing & Communication Technologies*, pp. 1-4, 2014.
- [28] C.-C. Yang, S.O. Prasher, J.-A. Landry and H.S. Ramaswamy, "Development of a Herbicide Application Map using Artificial Neural Networks and Fuzzy Logic", *Agricultural Systems*, Vol. 76, No. 2, pp. 561-574, 2003.
- [29] J.M. Guerrero, G. Pajares, M. Montalvo, J. Romeo and M. Guijarro, "Support Vector Machines for Crop/Weeds identification in Maize Fields", *Expert Systems with Applications*, Vol. 39, No. 12, pp. 11149-11155, 2012.
- [30] H. Tamura, S. Mori and T. Yamawaki, "Textural Features corresponding to Visual Perception", *IEEE Transactions on Systems, Man and Cybernetics*, Vol. 8, No. 6, pp. 460-472, 1978.
- [31] R.M. Haralick, K. Shanmugam and I. Dinstein, "Textural Features for Image Classification", *IEEE Transactions on Systems, Man and Cybernetics*, Vol. 3, No. 6, pp. 610-621, 1973.